

# Comparison of $^{99m}\text{Tc}$ - and $^{18}\text{F}$ -Ubiquicidin Autoradiography to Anti-*Staphylococcus aureus* Immunofluorescence in Rat Muscle Abscesses

Dagmar Salber<sup>1</sup>, Johannes Gunawan<sup>2</sup>, Karl-Josef Langen<sup>3</sup>, Eva Fricke<sup>2</sup>, Peter Klauth<sup>4</sup>, Wolfgang Burchert<sup>2</sup>, and Sijte Zijlstra<sup>2</sup>

<sup>1</sup>C. & O. Vogt Institute of Brain Research, University Hospital Düsseldorf, Düsseldorf, Germany; <sup>2</sup>Institute of Radiology, Nuclear Medicine, and Molecular Imaging, Heart and Diabetes Centre North Rhine-Westphalia, Bad Oeynhausen, Germany; <sup>3</sup>Institute of Neuroscience and Biophysics, Medicine Research Center Jülich, Jülich, Germany; and <sup>4</sup>Institute of Chemistry and Dynamics, Geosphere-Agrosphere Research Center, Jülich, Germany

$^{99m}\text{Tc}$ -ubiquicidin (UBI) 29-41 is under clinical evaluation for discrimination between bacterial infection and unspecific inflammation. We compared the distribution of  $^{99m}\text{Tc}$ -UBI 29-41, the potential PET tracers  $^{18}\text{F}$ -UBI 29-41 and  $^{18}\text{F}$ -UBI 28-41, and  $^3\text{H}$ -deoxyglucose (DG) in rat muscle abscesses to that of anti-*Staphylococcus aureus* immunofluorescent imaging. **Methods:** Calf abscesses were induced in 15 CDF-Fischer rats after inoculation of *Staphylococcus aureus*. One to 6 d later, either  $^{18}\text{F}$ -UBI 29-41 and  $^3\text{H}$ -DG ( $n = 5$ ) or  $^{18}\text{F}$ -UBI 28-41 and  $^3\text{H}$ -DG ( $n = 6$ ) or  $^{99m}\text{Tc}$ -UBI 29-41 and  $^3\text{H}$ -DG ( $n = 4$ ) were injected simultaneously. Dual-tracer autoradiography of the abscess area was compared with the distribution of bacteria and macrophages. **Results:** The UBI derivatives exhibited increased uptake in the abscess area that partly matched  $^3\text{H}$ -DG uptake and macrophage infiltration but showed no congruity with areas that were highly positive for bacteria. **Conclusion:** A specific binding of UBI derivatives to *Staphylococcus aureus* in vivo could not be confirmed in this study.

**Key Words:** bacterial infections; ubiquicidin;  $^{99m}\text{Tc}$ -UBI 29-41;  $^{18}\text{F}$ -UBI 29-41;  $^{18}\text{F}$ -UBI 28-41; autoradiography; *S. aureus*

J Nucl Med 2008; 49:995–999

DOI: 10.2967/jnumed.108.050880

**D**ifferentiation between infectious and noninfectious inflammation is a frequent problem in several clinical settings, and differentiation with MRI is difficult (1). One example is the discrimination of Charcot's neuroarthropathy and osteomyelitis in the diabetic foot (2). Early diagnosis of osteomyelitis is essential because it may result in less mutilating therapy.

The antimicrobial peptide  $^{99m}\text{Tc}$ -labeled ubiquicidin (UBI) 29-41 is a promising tracer for differentiation between

infectious and noninfectious inflammation (3,4).  $^{99m}\text{Tc}$ -UBI 29-41 binds to the negatively charged groups present on the bacterial cell envelope by electrostatic interaction, and there is some evidence that a specific mechanism is responsible for intrabacterial  $^{99m}\text{Tc}$ -UBI 29-41 accumulation (5).  $^{99m}\text{Tc}$ -UBI has been shown to accumulate at sites of muscular infections in mice and rabbits but not in inflamed aseptic muscular abscesses induced by lipopolysaccharides (6). Initial clinical studies have confirmed the experimental findings (3,7). In this study, we compared the autoradiographic distribution of  $^{99m}\text{Tc}$ -UBI 29-41 in experimental abscesses with the distribution of bacteria as depicted by immunofluorescent imaging using anti-*Staphylococcus aureus* antibodies. Furthermore, we included 2 different  $^{18}\text{F}$ -labeled UBI derivatives in the evaluation in order to transfer such investigations to PET. Dual-tracer autoradiography allowed the comparison to  $^3\text{H}$ -deoxyglucose uptake as a reference.

## MATERIALS AND METHODS

### Radiopharmaceuticals

$^{99m}\text{Tc}$ -labeling of UBI 29-41 (Thr-Gly-Arg-Alu-Lys-Arg-Met-Gln-Tyr-Asn-Arg-Arg) was mediated via complexation with  $^{99m}\text{Tc}$ -sodium pertechnetate (6) and  $^{18}\text{F}$  labeling of UBI 29-41 and UBI 28-41 via chemical connection of *N*-succinimidyl-4- $^{18}\text{F}$ -fluorobenzoate and the lysine group of UBI as described previously (8). Both compounds had a specific activity of more than 35 TBq/mmol. Tracer stability was confirmed by thin-layer chromatography or high-pressure liquid chromatography.  $^3\text{H}$ -deoxyglucose (DG) was obtained commercially (Amersham Biosciences Europe GmbH) with a specific radioactivity of 3 TBq/mmol.

### Animal Experiments

Fifteen male Fischer CDF rats (8–12 wk old; weight range, 150–410 g; Charles River Wiga) were examined in this study. The experiments were approved by the district government according to the German Law on the Protection of Animals (Cologne/Germany no. 50.203.2-KFA 5/03).

The animals were kept under standard conditions with free access to food and water. The animals were sedated in an isoflurane atmosphere (2%–5%) and anesthetized with an intra-

Received Jan. 19, 2008; revision accepted Feb. 18, 2008.

For correspondence or reprints contact: Karl-Josef Langen, Institute of Neuroscience and Biophysics-Medicine, Research Center Jülich, D-52425 Jülich, Germany.

E-mail: k.j.langen@fz-juelich.de

COPYRIGHT © 2008 by the Society of Nuclear Medicine, Inc.

**TABLE 1**  
Data on <sup>18</sup>F-UBI 29-41 in Animals with Calf Abscesses

Rat no.	Interval* (d)	Time† (min)	<sup>18</sup> F-UBI 29-41 uptake			<sup>3</sup> H-DG uptake		
			SUV <sub>max</sub> , abscess	SUV, muscle	L/M	SUV <sub>max</sub> , abscess	SUV, muscle	L/M
1	6	60	1.2	0.2	6.0	2.4	0.4	6.0
2	6	60	1.2	0.3	4.0	3.7	0.6	6.2
3	5	60	0.8	0.2	4.0	8.7	0.4	21.8
4	2	40	1.4	0.3	4.7	7.0	0.5	14.0
5	2	30	1.8	0.4	4.5	5.2	0.3	17.3
Mean			1.3‡	0.3	4.6‡	5.4	0.4	13.1
SD			0.4	0.1	0.8	2.5	0.1	6.9

\*After inoculation of *Staphylococcus aureus*.

†After injection of <sup>18</sup>F-UBI 29-41.

‡P < 0.01 vs. <sup>3</sup>H-DG.

L/M = lesion-to-muscle ratio.

peritoneal injection of ketamine (100 mg/kg) and xylazine (10 mg/kg). One hundred microliters of a bacterial suspension (*Staphylococcus aureus*, clinical strain 10B [10<sup>7</sup> colony-forming units/mL]; Novartis Pharma, Inc.) were slowly injected into the calf muscle.

One to 6 d after induction of the abscesses, the animals were reanesthetized for tracer injection. Either 100 MBq of <sup>18</sup>F-UBI 29-41 and 10 MBq of <sup>3</sup>H-DG (n = 5, Table 1) or 100 MBq of <sup>18</sup>F-UBI 28-41 and 10 MBq of <sup>3</sup>H-DG (n = 6, Table 2) or 100 MBq of <sup>99m</sup>Tc-UBI 29-41 and 10 MBq of <sup>3</sup>H-DG (n = 4, Table 3) were injected via a jugular vein in each animal. In most animals, the tracers were injected simultaneously; in some animals, the UBI derivatives were injected 20–30 min after injection of <sup>3</sup>H-DG. One hour after <sup>3</sup>H-DG injection, the animals were sacrificed and the calf muscles were removed immediately and frozen in 2-methylbutane at –50°C. Twenty-micrometer-thick sections of the abscess-bearing muscle were generated using a cryostat microtome (CM 3050; Leica Mikrosysteme Vertrieb GmbH).

#### Autoradiography

Sections of the muscle were placed on phosphor imaging plates (Raytest-Fuji) along with industrial tritium activity standards (Microscales; Amersham Biosciences) for <sup>3</sup>H-studies and with calibrated <sup>18</sup>F liver paste standards made in-house. The signal

from the different isotopes was separated by the use of special imaging plates and exposition timing as described previously (9). Quantitative autoradiograms were generated (Bq/mg of wet weight of the tissue) using the known radioactivity concentrations of the standards. The autoradiograms were evaluated by circular regions of interest placed on areas with maximal tracer uptake in the area of the abscesses (size, 2.9 ± 2.4 mm<sup>2</sup>) and an area of unaffected muscle tissue (size, 2 mm<sup>2</sup>). Standardized uptake values (SUVs) were calculated by normalization of the average uptake (Bq/mg) in the regions of interest of maximal tracer uptake in the lesion (SUV<sub>max</sub>) and the average uptake in normal muscle tissue (background) to injected dose and body weight. Lesion-to-muscle ratios were calculated by dividing the SUV<sub>max</sub> in the lesion by the SUV in normal tissue.

#### Double Immunofluorescent Labeling and Histologic Staining

Double immunofluorescent labeling was performed on serial slices. *Staphylococcus aureus* in the abscess area was identified with a specific polyclonal rabbit antibody against soluble and structural antigens of the whole bacterium (1:500, ab20920; Abcam).

**TABLE 2**  
Data on <sup>18</sup>F-UBI 28-41 in Animals with Calf Abscesses

Rat no.	Interval* (d)	Time† (min)	<sup>18</sup> F-UBI 28-41 uptake			<sup>3</sup> H-DG uptake		
			SUV <sub>max</sub> , abscess	SUV, muscle	L/M	SUV <sub>max</sub> , abscess	SUV, muscle	L/M
6	5 d	30	1.2	0.2	6.0	4.0	0.4	10.0
7	4 d	30	3.4	0.8	4.3	6.5	1.0	6.5
8	6 d	40	0.3	0.1	2.0	3.4	0.4	8.5
9	4 d	60	3.0	0.2	15.0	4.9	0.4	12.3
10	1 d	60	2.8	0.9	3.1	5.5	2.0	2.8
11	1 d	60	3.0	0.3	10.0	4.9	0.5	9.8
Mean			2.3‡	0.4	6.9	4.9	0.8	8.3
SD			1.2	0.3	4.6	1.1	0.6	3.3

\*After inoculation of *Staphylococcus aureus*.

†After injection of <sup>18</sup>F-UBI 28-41.

‡P < 0.01 vs. <sup>3</sup>H-DG.

L/M = lesion-to-muscle ratio.

**TABLE 3**  
Data on  $^{99m}\text{Tc}$ -UBI 29-41 in Animals with Calf Abscesses

Rat no.	Interval* (d)	Time† (min)	$^{99m}\text{Tc}$ -UBI 29-41 uptake			$^3\text{H}$ -DG uptake		
			SUV <sub>max</sub> , abscess	SUV, muscle	L/M	SUV <sub>max</sub> , abscess	SUV, muscle	L/M
12	5	60	0.7	0.7	1.0	3.9	1.7	2.3
13	5	60	1.4	0.2	7.0	2.8	0.4	7.0
14	1	60	1.9	0.4	4.8	3.4	0.4	8.5
15	1	60	0.6	0.3	2.0	3.4	0.6	5.7
Mean			1.2‡	0.4	3.7	3.4	0.8	5.9
SD			0.6	0.2	2.7	0.5	0.6	2.6

\*After inoculation of *Staphylococcus aureus*.  
†After injection of  $^{99m}\text{Tc}$ -UBI 29-41.  
‡ $P < 0.01$  vs.  $^3\text{H}$ -DG.  
L/M = lesion-to-muscle ratio.

Macrophages were demonstrated with mouse antirat CD68 monoclonal antibodies (1:50; Serotec MCA341R). As secondary antibodies, goat antirabbit Alexa Fluor 568 or goat antimouse Alexa Fluor 488 (1:300; Invitrogen) were used. In addition, tissue slices were histologically stained by toluidine blue or hematoxylin-eosin in serial slices.

#### Statistical Analysis

Values are expressed as mean  $\pm$  SD. The statistical methods used were the *t* test or Mann-Whitney rank sum test for group comparisons. Probability values of less than 0.05 were considered significant.

#### RESULTS

In all animals, distinct muscle abscesses could be generated. All UBI derivatives and  $^3\text{H}$ -DG exhibited focally increased uptake in the abscess area. The quantitative results for the different tracers are presented in Tables 1–3. Examples of the autoradiography of each UBI derivative in comparison to  $^3\text{H}$ -DG and anti-CD68 immunofluorescent imaging of

macrophages and *Staphylococcus aureus* are shown in Figures 1–3. The distribution pattern of the UBI derivatives partly matched  $^3\text{H}$ -DG uptake and macrophage infiltration but showed no clear congruity with areas that were highly positive for *Staphylococcus aureus*. The interval between inoculation of the bacteria and sacrifice of the animals varied from 1 to 6 d, with no obvious differences in the results.

#### DISCUSSION

This study was undertaken to further investigate specific binding of UBI derivatives to bacteria in vivo and to transfer this approach to PET using new  $^{18}\text{F}$ -labeled UBI derivatives. The results, however, did not confirm our expectations and challenge the concept of specific in vivo imaging of bacterial infections using UBI derivatives.  $^{99m}\text{Tc}$ -UBI 29-41 and the  $^{18}\text{F}$ -UBI derivatives exhibited variably increased uptake in the area of bacterial abscesses,

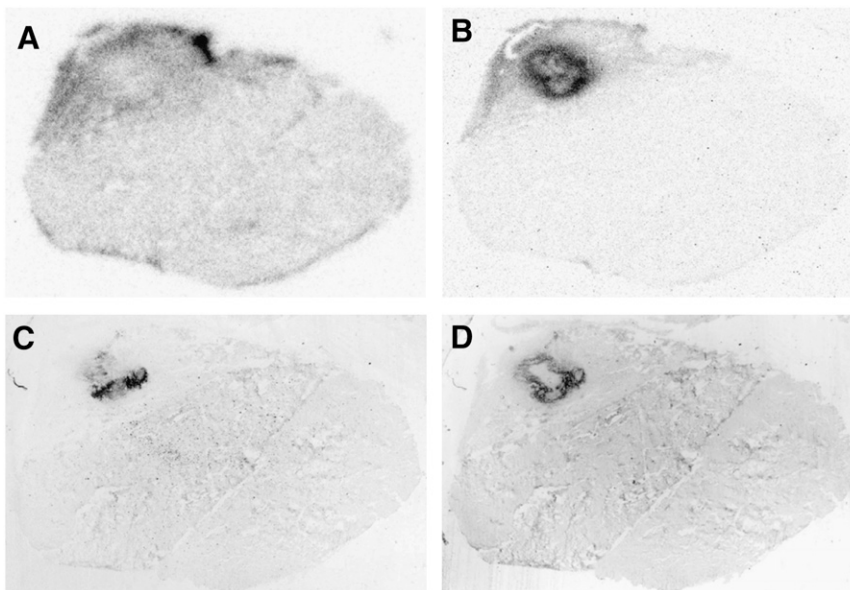


**FIGURE 1.** Tissue slices of calf muscle 5 d after abscess induction (rat 3):  $^{18}\text{F}$ -UBI 29-41 autoradiography (A),  $^3\text{H}$ -DG autoradiography (B), immunofluorescent imaging using antistaphylococcus antibodies (C), and immunofluorescent imaging using anti-CD68 antibodies (macrophages) (D). No congruity exists between  $^{18}\text{F}$ -UBI 29-41 uptake and bacterial distribution.  $^3\text{H}$ -DG uptake in abscess rim matches area of macrophage infiltration.

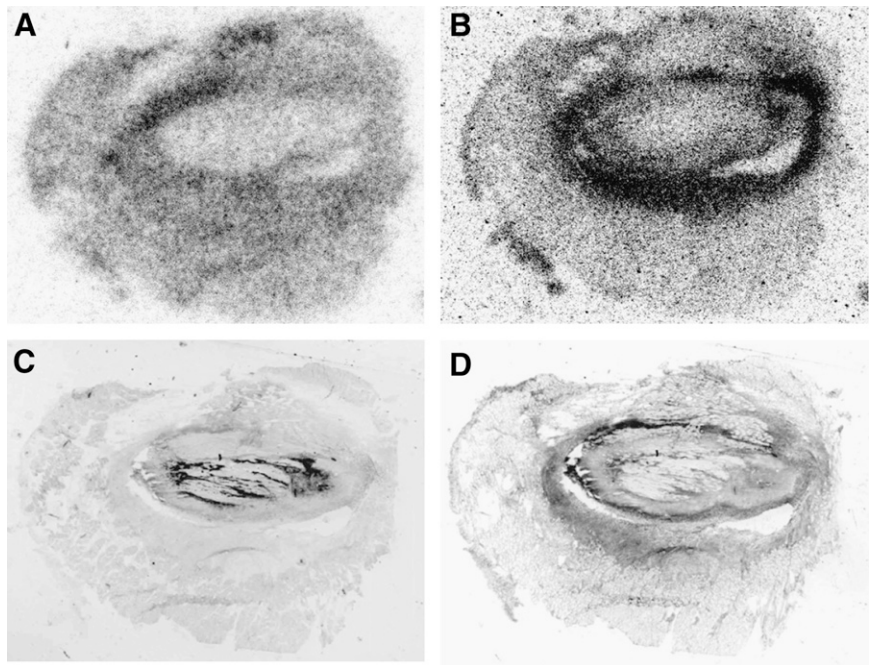


**FIGURE 2.** Tissue slices of calf muscle 4 d after abscess induction (rat 7):  $^{18}\text{F}$ -UBI 28-41 autoradiography (A),  $^3\text{H}$ -DG autoradiography (B), immunofluorescent imaging using anti-staphylococcus antibodies (C), and immunofluorescent imaging using anti-CD68 antibodies (macrophages) (D). Again, no congruity exists between  $^{18}\text{F}$ -UBI 28-41 uptake and bacterial distribution.  $^3\text{H}$ -DG uptake in abscess rim matches area of macrophage infiltration.

but in no case was a clear congruity of tracer accumulation with the distribution of *S. aureus* observed.

Because our findings contradict several studies that have demonstrated a potential of  $^{99\text{m}}\text{Tc}$ -UBI 29-41 for specific detection of bacterial infections, the methodologic aspects of this study need to be discussed. So far, the specific binding of  $^{99\text{m}}\text{Tc}$ -UBI 29-41 to bacteria has been demonstrated either in vitro or by external  $\gamma$ -camera imaging of animals or humans after intravenous injection of the tracer. To the best of our knowledge, no study has demonstrated an immediate binding of  $^{99\text{m}}\text{Tc}$ -UBI 29-41 to bacteria in the tissue by autoradiography.

The in vitro binding of  $^{99\text{m}}\text{Tc}$ -UBI 29-41 has been reported to be  $34.3\% \pm 3.0\%$  (5). Corresponding values were approximately 15% for  $^{18}\text{F}$ -UBI 29-41 (8) and 37%–57% for  $^{18}\text{F}$ -UBI 28-41 (Sijtse Zijlstra, unpublished data, 2006) indicating that the  $^{18}\text{F}$ -labeled UBI derivatives have a potential similar to that of  $^{99\text{m}}\text{Tc}$ -UBI 29-41 for imaging bacterial infections.

One parameter that plays a role in the binding of UBI derivatives to bacteria in vivo is the timing of the imaging study after intravenous application of the tracer. In our study, animals were sacrificed between 30 and 60 min after injection of UBI derivatives—a time identical to that in

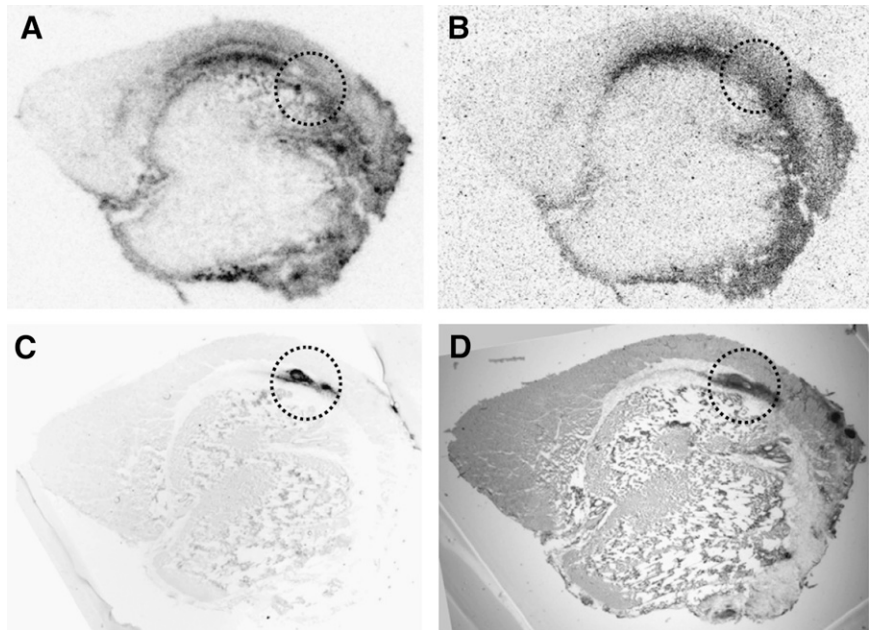


**FIGURE 3.** Tissue slices of calf muscle 1 d after bacterial inoculation (rat 14):  $^{99\text{m}}\text{Tc}$ -UBI 29-41 autoradiography (A),  $^3\text{H}$ -DG autoradiography (B), immunofluorescent imaging with anti-staphylococcus aureus antibodies (C), and hematoxylin-eosin staining (D). No congruity exists between  $^{99\text{m}}\text{Tc}$ -UBI 29-41 uptake and bacterial distribution.  $^3\text{H}$ -DG uptake is low in area with high bacterial density (dotted circle), which is also depicted with hematoxylin-eosin staining.

which maximal target-to-nontarget ratios have been reported in previous experimental and clinical studies using  $^{99m}\text{Tc}$ -UBI 29-41 (3,4,6,10).

Furthermore, the time between bacterial inoculation and sacrifice of the animals may influence the results. In previous studies, imaging was done at 24 or 48 h after inoculation of bacteria into the thigh muscle (7,10). In our study, the period after inoculation of bacteria ranged from 1 to 6 d, and the optimal time point for imaging after inoculation of the bacteria is unlikely to have been missed.

A more important constraint in our experiments may be the fact that the UBI derivatives could not bind to the bacteria because they were encapsulated in the center of the abscess or phagocytized by macrophages. In vitro experiments have shown that  $^{99m}\text{Tc}$ -UBI 29-41 binding to granulocytes with phagocytized bacteria was low and similar to that of granulocytes without bacteria, suggesting that at sites of infection, mainly extracellular bacteria are targeted (10). Phagocytosis or encapsulation of free bacteria, however, is a physiologic process that usually happens within hours, and it is questionable whether a tracer that can target only free bacteria in high concentrations is a sensitive marker of bacterial infections.

Another important aspect concerns the limited specificity of UBI derivatives. We found increased uptake of all UBI derivatives at sites within the abscess area that showed no binding of *S. aureus* antibodies. The binding correlated partly with  $^3\text{H}$ -DG accumulation, but the pattern of uptake was not consistent with macrophage infiltration, indicating unspecific binding of the UBI derivatives. Unspecific binding of  $^{99m}\text{Tc}$ -UBI 29-41 has also been reported in 1 patient with soft-tissue inflammation in whom cultures were negative for bacteria (8). On the basis of our evaluations of tissue staining, we are at present unable to provide a consistent hypothesis for the mechanisms of unspecific binding of the UBI derivatives.

Although our results do not support the expectation that UBI derivatives are promising tracers for the detection of bacterial infections, one cannot exclude the possibility that other mechanisms of binding that are specifically associated with bacterial infections may explain the results of previous studies. In that case, of the potential PET tracers tested in this study  $^{18}\text{F}$ -UBI 28-41 has to be considered to have the best

imaging characteristics. Because lesion-to-muscle ratios with this tracer were considerably higher than those with  $^{18}\text{F}$ -UBI 29-41 and  $^{99m}\text{Tc}$ -UBI 29-41, preference should be given to evaluations of this tracer in further studies.

## CONCLUSION

A specific binding of UBI derivatives to *Staphylococcus aureus* in vivo could not be confirmed in this study. Thus, the specificity of radiolabeled UBI derivatives for discrimination between bacterial infection and unspecific inflammation is questionable.

## ACKNOWLEDGMENTS

We thank Stephanie Klein, Dr. Gabriele Stoffels, and Norbert Hartwigsen for assistance in animal experiments and data evaluation.

## REFERENCES

1. Ledermann HP, Morrison WB. Differential diagnosis of pedal osteomyelitis and diabetic neuroarthropathy: MR imaging. *Semin Musculoskelet Radiol.* 2005;9:272–283.
2. Lipsky BA, Berendt AR, Deery HG, et al. Diagnosis and treatment of diabetic foot infections. *Plast Reconstr Surg.* 2006;117(suppl):212S–238S.
3. Akhtar MS, Qaisar A, Irfanullah J, et al. Antimicrobial peptide  $^{99m}\text{Tc}$ -ubiquicidin 29-41 as human infection-imaging agent: clinical trial. *J Nucl Med.* 2005;46:567–573.
4. Sarda-Mantel L, Saleh-Mghir A, Welling MM, et al. Evaluation of  $^{99m}\text{Tc}$ -UBI 29-41 scintigraphy for specific detection of experimental *Staphylococcus aureus* prosthetic joint infections. *Eur J Nucl Med Mol Imaging.* 2007;34:1302–1309.
5. Ferro-Flores G, Arteaga de Murphy C, Pedraza-López M, et al. In vitro and in vivo assessment of  $^{99m}\text{Tc}$ -UBI specificity for bacteria. *Nucl Med Biol.* 2003;30:597–603.
6. Welling MM, Lupetti A, Balter HS.  $^{99m}\text{Tc}$ -labeled antimicrobial peptides for detection of bacterial and *Candida albicans* infections. *J Nucl Med.* 2001;42:788–794.
7. Meléndez-Alafort L, Rodríguez-Cortés J, Ferro-Flores G, et al. Biokinetics of  $^{99m}\text{Tc}$ -UBI 29-41 in humans. *Nucl Med Biol.* 2004;31:373–379.
8. Zijlstra S, Gunawan J, Freytag C, Burchert W. Synthesis and evaluation of fluorine-18 labelled compounds for imaging of bacterial infections with PET. *Appl Radiat Isot.* 2006;64:802–807.
9. Salber D, Stoffels G, Pauleit D, et al. Differential uptake of O-(2- $^{18}\text{F}$ -fluoroethyl)-L-tyrosine, L- $^3\text{H}$ -methionine, and  $^3\text{H}$ -deoxyglucose in brain abscesses. *J Nucl Med.* 2007;48:2056–2062.
10. Nibbering PH, Welling MM, Paulusma-Annema A, Brouwer CP, Lupetti A, Pauwels EK.  $^{99m}\text{Tc}$ -Labeled UBI 29-41 peptide for monitoring the efficacy of antibacterial agents in mice infected with *Staphylococcus aureus*. *J Nucl Med.* 2004;45:321–326.